J|A|C|S
ARTICLES
Published on Web 02/04/2006

Phase Behavior in Thin Films of Confined Colloid−Polymer Mixtures

Chun-lai Ren and Yu-qiang Ma*

Contribution from the National Laboratory of Solid State Microstructures, Nanjing University, Nanjing 210093, China

Received November 6, 2005; E-mail: myqiang@nju.edu.cn

Abstract: Using self-consistent-field and density-functional theories, we first investigate colloidal self-assembly of colloid−polymer films confined between two soft surfaces grafted by polymers. With increasing colloidal concentrations, the film undergoes a series of transitions from disordered liquid → sparse square → hexagonal (or mixed square-hexagonal) → dense square → cylindrical structures in a plane, which results from the competition between the entropic elasticity of polymer brushes and the steric packing effect of colloidal particles. A phase diagram displays the stable regions of different in-layer ordering structures as the colloidal concentration is varied and layering transitions as the polymer-grafted density is decreased. Our results show a new control mechanism to stabilize the ordering of structures within the films.

Introduction

Dispersions of colloidal particles in polymer solutions are the basic ingredients of a wide variety of systems which are essential to life and major industries.[1,2] In particular, assembling colloidal nanoparticles into ordered structures[3−18] is important to the fabrication of nanomaterials with high performance in size-dependent optical, electrical, and mechanical properties. A major challenge in this field is to assemble monodispersed colloids into highly ordered structures with well-controlled sizes and shapes. Usually, the dispersed structures depend on the effective interaction between the colloidal particles themselves and between the colloidal particles and their surroundings. For example, the interaction between colloidal particles in a solution of nonadsorbing polymers is influenced by entropic excluded-volume (depletion) forces, which were first recognized theoretically by Askura and Oosawa,[19] and thus a monodisperse colloidal system may typically crystallize into a close-packed structure or a body-centered-cubic lattice with high symmetry.

Thin films made of mixtures of polymer and colloidal particles can exhibit interesting structures which are particularly useful for nano(bio)technology, for applications ranging from nanopatterning/lithography to changing surface properties. Surface confinement modifies the bulk behavior of the system by breaking the symmetry of the structure, and therefore it can be used to make low-dimensional ordering films. For nanosized colloidal particles, the confinement of the suspension is a straightforward approach for the formation of colloidal crystals. For example, when the colloid−polymer mixtures are sandwiched between two parallel hard surfaces, layered structures may form, but the in-plane structure of the particles is always uniform or close-packed. Polymer brushes grafted to surfaces can modify the properties of the surface,[20−22] which has many applications in colloidal stabilization and biocompatibility. Interestingly, the grafted polymer chains may lead to a long-ranging repulsive force between the particles, which stabilizes the ordering of the nanosized particles and controls the symmetry of the structure formed in a desired direction. Such control is required for a wide range of applications based on the structure-dependent optical, electrical, and mechanical properties of the colloidal crystals. It has been noted[23−27] that thin films made of charged colloidal suspensions have various layered crystalline states if the film is confined between two parallel plates which

(1) Russel, W. B.; Saville, D. A.; Schowalter, W. R. *Colloidal Dispersions*; Cambridge University Press: Cambridge, 1989.
(2) Fuchs, M.; Schweizer, K. S. *J. Phys.: Condens. Matter* **2002**, *14*, R239.
(3) Whitesides, G. W.; Boncheva, M. *Proc. Natl. Acad. Sci.* **2002**, *99*, 4769.
(4) Liu, Z.; Pappacena, K.; Cerise, J.; Kim, J.; Durning, C. J.; O'Shaughnessy, B.; Levicky, R. *Nano. Lett.* **2002**, *2*, 219.
(5) Zhu, J.; Li, M.; Rogers, R.; Meyer, W.; Ottewill, R. H.; STS-73 Space Shuttle Crew; Russel, W. B.; Chaikin, P. M. *Nature* **1997**, *387*, 883.
(6) van Blaaderen, A.; Ruel, R.; Wiltzius, P. *Nature* **1997**, *385*, 321.
(7) Yethiraj, A.; van Blaaderen, A. *Nature* **2003**, *421*, 513.
(8) Ramos, L.; Lubensky, T. C.; Dan, N.; Nelson, P.; Weitz, D. A. *Science* **1999**, *286*, 2325.
(9) Lin, K. H.; Crocker, J. C.; Prasad, V.; Schofield, A.; Weitz, D. A.; Lubensky, T. C.; Yodh, A. G. *Phys. Rev. Lett.* **2000**, *85*, 1770.
(10) Lin, Y.; Boker, A.; He, J. B.; Sill, K.; Xiang, H. Q.; Abetz, C.; Li, X. F.; Wang, J.; Emrick, T.; Long, S.; Wang, Q.; Balazs, A. C.; Russell, T. P. *Nature* **2005**, *434*, 55.
(11) Lin, Y.; Skaff, H.; Emrick, T.; Dinsmore, A. D.; Russell, T. P. *Science* **2003**, *299*, 226.
(12) Bechinger, C. *Curr. Opin. Colloid Interface Sci.* **2002**, *7*, 204.
(13) Wang, D. Y.; Mohwald, H. *J. Mater. Chem.* **2004**, *14*, 459.
(14) Xia, Y.; Yin, Y.; Lu, Y.; Mclellan, J. *Adv. Funct. Mater.* **2002**, *14*, 605.
(15) Yin, Y.; Lu, Y.; Gates, B.; Xia, Y. *J. Am. Chem. Soc.* **2001**, *123*, 8718.
(16) Yin, Y.; Xia, Y. *Adv. Mater.* **2002**, *14*, 605.
(17) Kim, E.; Xia, Y.; Whitesides, G. M. *Adv. Mater.* **1996**, *8*, 245.
(18) Yang, P.; Rivzi, A. H.; Messer, B.; Chemlka, B. F.; Whitesides, G. M.; Stucky, G. D. *Adv. Mater.* **2001**, *13*, 427.
(19) Asakura, S.; Oosawa, F. *J. Polym. Sci.* **1958**, *33*, 183.
(20) Milner, S. T. *Science* **1991**, *251*, 905.
(21) (a) Satulovsky, J.; Carignano, M. A.; Szleifer, I. *Proc. Natl. Acad. Sci.* **2000**, *97*, 9037. (b) Currie, E. P. K.; Norde, W.; Cohen Stuart, M. A. *Adv. Colliod Interface Sci.* **2003**, *100−102*, 205.
(22) Ren, C. L.; Chen, K.; Ma, Y. Q. *J. Chem. Phys.* **2005**, *122*, 154904.
(23) Murray, C. A.; Grier, D. G. *Annu. Rev. Phys. Chem.* **1996**, *47*, 421.
(24) Messina, R.; Löwen, H. *Phys. Rev. Lett.* **2003**, *91*, 146101.
(25) Schmidt, M.; Löwen, H. *Phys. Rev. Lett.* **1996**, *24*, 4552.
(26) Wasan, D. T.; Nikolov, A. D. *Nature* **2003**, *423*, 156.
(27) Henderson, D.; Trokhymchuk, A.; Nikolov, A.; Wasan, D. T. *Ind. Eng. Chem. Res.* **2005**, *44*, 1175.

repel the colloidal particles. Here, we show that, for colloid−polymer mixtures, using polymer brush surfaces is an effective way of changing the in-plane structure of the colloidal film.

The purpose of the present article is to demonstrate a novel way of spatially organizing the colloid dispersions in polymer solutions confined between two polymer-grafted plates. We find that, with the deformation of grafted chains by the particles, the deformed brushes can exert an additional interaction between nanosized colloidal particles, which stabilizes the formation of low-symmetric ordering structures of colloids. Such a brush-mediated colloidal effective interaction will compete with steric (center-force) effects of colloids, which may generate structures with more complicated lattice symmetries that undergo symmetry-changing transitions in-plane. In the present model, layering structures are formed due to confinement, and more importantly, in-layer structural transitions are observed, depending upon the colloidal concentration and the polymer-grafted density. The results are summarized in a phase diagram displaying the stability regions of self-assembled ordering phases as functions of the colloidal concentration and the polymer-grafted density. The proposed approach is physically achievable for the generation of novel ordered structures. A successful example indicating the importance of such a self-assembly mechanism is the recent experimental verification[10] of the predicated phase behavior of the copolymer/particle mixtures in confined geometries.[28,29] Another motivation of the present work is the fact that, although many experiments have demonstrated the success of fabricating self-assembled nanostructures, an understanding of the physical mechanism that drives the self-assembly of the colloidal particles in confined geometries is still lacking.[28−31]

Model Details

We consider a colloid suspension confined between two planar plates separated by a distance L_z along the z-axis. The two plates which are grafted with n_{br} A-type homopolymer chains are horizontally placed in the xy-plane and mechanically fixed at $z = 0$ and $z = L_z$, respectively. All B-type free homopolymer chains in solutions are flexible, with the same polymerization N and statistical length a, and incompressible with a segment volume ρ_0^{-1} as in A-type grafted chains. The volume of the system V is $L_xL_yL_z$, where L_x and L_y are the lateral lengths of the surfaces. The grafting density is defined as $\sigma = n_b/(2L_xL_y)$; the average volume fraction of grafted chains is $\phi_b = n_bN\rho_0^{-1}/V$, that of the colloid is $\phi_c = (1 - \phi_b)\psi_c$, where ψ_c is the colloidal concentration of the colloid−polymer mixture, and that of the free polymer is $\phi_p = 1 - \phi_b - \phi_c$. Recently, the self-consistent-field theory (SCFT) has been proven to be powerful in calculating equilibrium morphologies in polymeric systems,[32−42] while colloidal particles can be treated by density-functional theory (DFT)[41−44] to account for steric packing effects of particles. In our calculation, we use the hybrid SCFT/DFT approach developed in refs 41 and 42, and the free energy F for the present system is given by

$$\frac{NF}{\rho_0 k_B TV} = -\phi_b \ln\left(\frac{Q_b}{V\phi_b}\right) - \phi_p \ln\left(\frac{Q_p}{V\phi_p}\right) - \frac{\phi_c}{\alpha}\ln\left(\frac{Q_c\alpha}{V\phi_c}\right) + \frac{1}{V}\int d\mathbf{r}[\chi_{bp}N\varphi_b(\mathbf{r})\varphi_p(\mathbf{r}) + \chi_{bc}N\varphi_b(\mathbf{r})\varphi_c(\mathbf{r}) + \chi_{pc}N\varphi_p(\mathbf{r})\varphi_c(\mathbf{r}) - W_b(\mathbf{r})\varphi_b(\mathbf{r}) - W_p(\mathbf{r})\varphi_p(\mathbf{r}) - W_c(\mathbf{r})\rho_c(\mathbf{r}) - \xi(\mathbf{r})(1 - \varphi_b(\mathbf{r}) - \varphi_p(\mathbf{r}) - \varphi_c(\mathbf{r})) + \rho_c\Psi_{hs}(\bar{\varphi}_c)] \quad (1)$$

where k_B is the Boltzmann constant and T is the temperature. α is the volume ratio of the colloidal particle of radius R to polymer chain: $\alpha = v_R\rho_0/N$, where $v_R = (4/3)\pi R^3$. $\varphi_b(\mathbf{r})$, $\varphi_p(\mathbf{r})$, and $\varphi_c(\mathbf{r})$ are the local volume fractions of brushes, free polymers, and colloids, respectively. $\xi(\mathbf{r})$ is the potential field that ensures the incompressibility of the system for dense colloid−polymer mixtures. ρ_c stands for the particle center distribution, and the local particle volume fraction is then given by $\varphi_c(\mathbf{r}) = (\alpha/v_R)\int_{|\mathbf{r}'|<R} d\mathbf{r}'\ \rho_c(\mathbf{r} + \mathbf{r}')$.[41,42] The χ's are the Flory interaction parameters between the different chemical species. $Q_b = \int d\mathbf{r}\ q_1(\mathbf{r},s)\ q_1^+(\mathbf{r},s)$ and $Q_p = \int d\mathbf{r}\ q_2(\mathbf{r},1)$ are single-chain partition functions for brushes and free polymers under the self-consistent fields $W_b(\mathbf{r})$ and $W_p(\mathbf{r})$, respectively. $Q_c = \int d\mathbf{r}\ \exp[-W_c(\mathbf{r})]$ is the partition function for colloids under the self-consistent-field $W_c(\mathbf{r})$. The end-segment distribution functions $q_i(\mathbf{r},s)$ and $q_i^+(\mathbf{r},s)$ represent the probability of finding segment s at position $\mathbf{r}$, respectively, from two distinct ends of chains, which satisfy the modified diffusion equations $\partial q_i/\partial s = (a^2N/6)\nabla^2 q_i - W_i(\mathbf{r})q_i$ and $\partial q_i^+/\partial s = -(a^2N/6)\nabla^2 q_i^+ + W_i(\mathbf{r})q_i^+$. For the grafted chains in the field $W_b(\mathbf{r})$, the initial condition is $q_1(x, y, z = 0$ or $L_z, 0) = 1$, $q_1(x, y, z \neq 0$ or $L_z, 0) = 0$, and $q_1^+(x, y, z, 1) = 1$, which means that the end of the brush chains can move on the plates, although the total number of chains on surfaces is fixed. These have been called liquid brushes, in contrast to solid brushes where the immobile chains are anchored onto the surfaces.[45] Here we consider the liquid brush case because of its wide-ranging applications in colloidal and biological systems. For free polymers, the initial condition is $q_2(x, y, z, 0) = 1$. The last term in eq 1 is the DFT term,[43] accounting for the steric interaction between particles, and the excess free energy $\Psi(\bar{\varphi}_c)$ per particle is from the Carnahan−Starling function,[44] $\Psi_{hs}(x) = (4x - 3x^2)/(1 - x)^2$, with the weighted particle density $\bar{\varphi}_c(\mathbf{r})$,[41] $\bar{\varphi}_c(\mathbf{r}) = (\alpha/v_{2R})\int_{|\mathbf{r}'|<2R} d\mathbf{r}'\rho_c(\mathbf{r} + \mathbf{r}')$, where v_{2R} is the volume of a sphere of radius $2R$.

By minimizing the free energy in eq 1 with respect to $W_b(\mathbf{r})$, $W_p(\mathbf{r})$, $W_c(\mathbf{r})$, $\varphi_b(\mathbf{r})$, $\varphi_p(\mathbf{r})$, $\varphi_c(\mathbf{r})$, and $\xi(\mathbf{r})$, we obtain a set of self-consistent equations describing the equilibrium morphology of films, which can be solved numerically by the real-space combinatorial screening algorithm of Drolet and Fredrickson.[32,33] Free energy minimization of the system with respect to the selected simulation sizes is performed.[46] We fix $N = 100$, $L_z = 50a$, and the colloid diameter $2R = 0.6R_0$, where $R_0 \equiv aN^{1/2}$ characterizes the natural size of free polymers (typically 10−100 nm). On the other hand, on the basis of the assumptions that the interaction between different chemical species should be small enough and polymer brushes are chemically neutral to free polymers and colloids, we choose the Flory−Huggins interaction parameters $\chi_{pc}N = 5.0$ and $\chi_{bp}N = \chi_{bc}N = 8.0$. All the sizes are in units of a.

Results and Discussion

We first explore the formation of ordered structures of colloidal crystallization in confined colloidal solution film. Figure 1 shows a series of particle-dispersed morphologies of

(28) Lee, J. Y.; Shou, Z.; Balazs, A. C. *Phys. Rev. Lett.* **2003**, *91*, 136103.
(29) Lee, J. Y.; Shou, Z.; Balazs, A. C. *Macromolecules* **2003**, *36*, 7730.
(30) Lee, J. Y.; Buxton, G. A.; Balazs, A. C. *J. Chem. Phys.* **2004**, *121*, 5531.
(31) Buxton, G. A.; Lee, J. Y.; Balazs, A. C. *Macromolecules* **2003**, *36*, 9631.
(32) Drolet, F.; Fredrickson, G. H. *Phys. Rev. Lett.* **1999**, *83*, 4317.
(33) Drolet, F.; Fredrickson, G. H. *Macromolecules* **2001**, *34*, 5317.
(34) Schmid, F. *J. Phys.: Condens. Matter* **1998**, *10*, 8105.
(35) Matsen, M. W.; Schick, M. *Phys. Rev. Lett.* **1994**, *72*, 2660.
(36) Petera, D.; Muthukumar, M. *J. Chem. Phys.* **1998**, *109*, 5101.
(37) Matsen, M. W.; Bates, F. S. *J. Chem. Phys.* **1997**, *106*, 2436.
(38) Maniadis, P.; Thompson, R. B.; Rasmussen, K.; Lookman, T. *Phys. Rev. E* **2004**, *69*, 031801.
(39) Muller, M. *Phys. Rev. E* **2002**, *65*, 030802.
(40) Geisinger, T.; Muller, M.; Binder, K. *J. Chem. Phys.* **1999**, *111*, 5241.
(41) Thompson, R. B.; Ginzburg, V. V.; Matsen, M. W.; Balazs, A. C. *Science* **2001**, *292*, 2469.
(42) Thompson, R. B.; Ginzburg, V. V.; Matsen, M. W.; Balazs, A. C. *Macromolecules* **2002**, *35*, 1060.
(43) Tarazona, P. *Mol. Phys.* **1984**, *52*, 81.
(44) Carnahan, N. F.; Starling, K. E. *J. Chem. Phys.* **1969**, *51*, 635.
(45) Subramanian, G.; Williams, D. R. M.; Pincus, P. A. *Macromolecules* **1996**, *29*, 4045.
(46) Bohbot-Raviv, Y.; Wang, Z. G. *Phys. Rev. Lett.* **2000**, *85*, 3428.

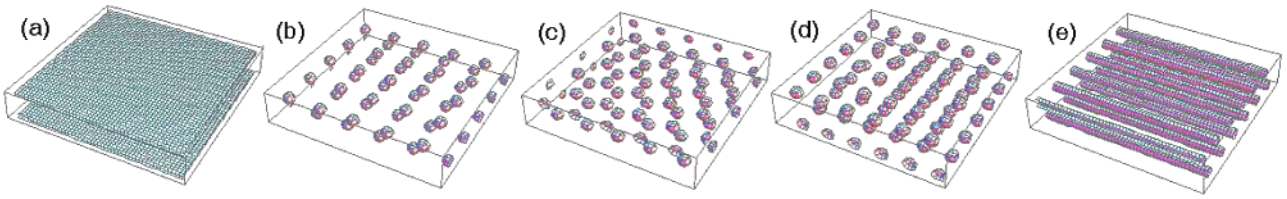

Figure 1. Distributions of colloidal particles with increasing colloidal concentration for the brush density $\sigma = 0.2$ and $L_x = L_y = 50$. The colloids can form in-layer sparse square, hexagonal, dense square, and cylindrical structures, and are arranged into two layers in an alternating manner. (a) $\psi_c = 0.29$, (b) $\psi_c = 0.30$, (c) $\psi_c = 0.35$, (d) $\psi_c = 0.38$, and (e) $\psi_c = 0.45$.

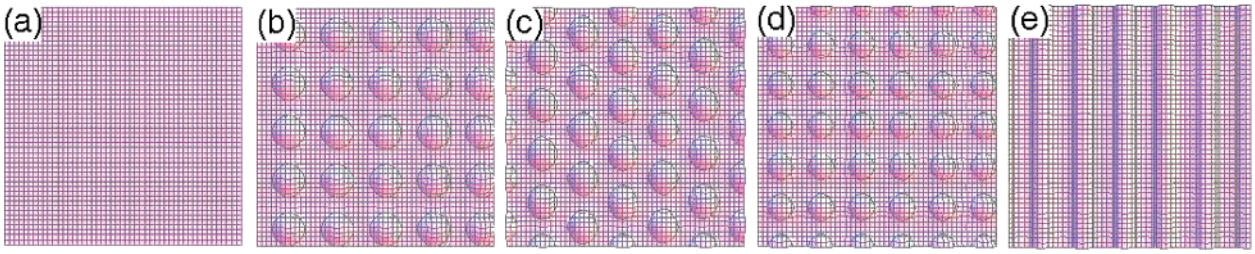

Figure 2. Top views of the density profiles of polymer brushes. Parameters are the same as in Figure 1.

varying colloidal concentration ψ_c, and Figure 2 shows the top views of profiles for polymer brushes grafted to one of the plates. We observe the formation of two layers of colloidal particles which are close to the polymer brush. When the colloidal concentration is small (for example, $\psi_c = 0.29$, as in Figure 1a), colloids distribute uniformly in the plane, and the interfaces with the brush remain level (Figure 2a). With increasing colloidal concentration, colloidal crystallization may occur, and inhomogeneous colloidal distribution will lead to the deformation of polymer brushes: caving where colloids exist and protruding where they do not. The deformed brushes prefer to stabilize the formation of low symmetric ordering structures of colloids, and with increasing colloidal concentration, the particles grow anisotropically along a one-dimensional direction.[47] We see from Figure 1b−e that, for different colloidal concentrations, colloids can assemble into sparse square, hexagonal, dense square, and cylindrical structures, depending on the competition between the entropic effect of the polymer brushes and the steric packing effect of the particles. Figure 2b−e shows the shapes of deformed brush surfaces corresponding to the respective colloidal structures. When $\psi_c = 0.30$, the average distance between colloidal particles is relatively large, and thus the brush-mediated interaction between colloids dominates over the steric packing effect of colloids, leading to in-layer square structures for possibly large conformational entropy of polymer brushes (Figure 2b). When $\psi_c = 0.35$, the stable state becomes hexagonal (Figures 1c and 2c), indicating that colloidal steric packing effects dominate. However, a dense square structure appears at $\psi_c = 0.38$ (Figure 1d), due to the requirement of entropic elastic release of deformed brushes. Further increase of colloids greatly limits the conformational space of brushes, and the entropy of brushes may be released by the formation of a cylindrical arrangement of colloids, because in this case, the free ends of grafted chains can at least move freely between parallel cylinders, as shown in Figures 1e and 2e when $\psi_c = 0.45$. Figure 2 shows that the polymer brush is soft, and its density variation changes with the colloidal concentration. The range of the density variation in the direction perpendicular to the substrate is comparable to the size of the colloidal particles. The brush density close to the substrate remains unchanged with varying colloidal concentrations for a given grafting density.

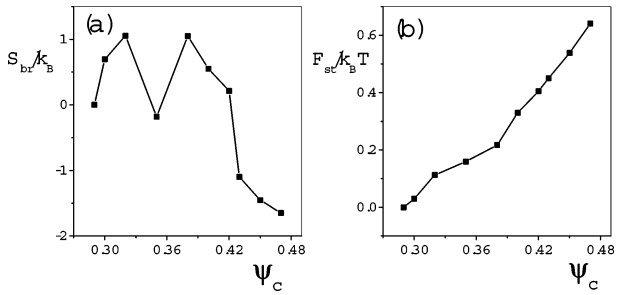

Figure 3. (a) Grafted-chain entropy (S_{br}/k_B) vs the colloidal concentration. (b) Averaged steric energy per colloidal particle (F_{st}/k_BT) vs the colloidal concentration.

Figure 3a shows the entropy of a grafted chain as a function of the colloidal concentration ψ_c. We set the grafted chain's entropy $S_{br}/k_B = 0$, when the dispersion of colloidal particles is uniform in the plane ($\psi_c = 0.29$). The entropy of polymer brushes, with colloidal concentrations varying from $\psi_c = 0.29$ to $\psi_c = 0.32$, increases with the formation of colloidal square structures. However, the brush entropy curve suddenly decreases with the influence of steric interaction of colloids, and a hexagonal structure is formed when $\psi_c = 0.35$. With further increase of colloidal concentration, the deformed brushes begin to dominate over the steric energy of colloids again, and the result is a release of the conformational space of brushes with the gradual formation of square structures. The brush entropy arrives at the maximum at $\psi_c = 0.38$, corresponding to the formation of dense square lattice structure (Figure 1d). After that, brush entropy decreases with increasing colloidal concentrations, and colloidal cylindrical structures begin to form. The complete cylindrical structure appears at $\psi_c = 0.42$, and remains unchanged even for larger colloidal concentrations. Usually, the entropic gain or loss due to the conformational change of polymer chains may signify the structural transitions of the polymeric system. For example, Balazs and co-workers[41,42] studied an AB diblock−nanoparticle composite in which the particles and diblock chains form spatially periodic structures. They observed a similar behavior of A-block entropic free

(47) Kim, J. U.; O'Shaughnessy, B. *Phys. Rev. Lett.* **2002**, *89*, 238301.

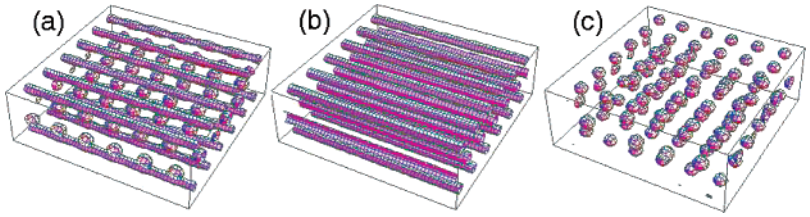

Figure 4. Formation of three-layer structures: (a) spherical-cylindrical mixture when $\sigma = 0.17$ and $\psi_c = 0.36$; (b) cylindrical structure when $\sigma = 0.17$ and $\psi_c = 0.42$; and (c) spherical structure when $\sigma = 0.16$ and $\psi_c = 0.32$.

energy when the volume fraction of the particles was increased.[41] In their work, however, the conformational entropy of the A-block showed only the stretching and compressing of the A-block chains along the chain direction, because they considered the formation of spatially periodic structures in two-dimensional copolymer−nanoparticle composites in the plane of the polymer chains. In contrast, in the present three-dimensional confined mixtures of colloidal particles and free homopolymer chains, we emphasize a control mechanism in the lateral direction of the colloidal suspension driven by the deformed chains in the polymer brush. Actually, the entropic free energy in Figure 3a depicts the shape changes of the brush surface (Figure 2) during the variation of the colloidal concentration for a given grafting density $\sigma = 0.2$. The configurational entropy contribution of the grafted chains originates from the free ends of the brushes which are comparable in size to the colloidal particles, since the bottom part of the chains close to the substrate is strongly stretched and remains nearly unchanged with varying colloidal concentration for a fixed grafting density. This means that the entropic effect of the brushes deformed by the particles comes mainly from the lateral conformation fluctuations of the free chain ends, and that the averaged conformational entropy contribution of the polymer brushes along the chain-stretching direction can be ignored. Such an entropic effect competes with the steric packing effect of the particles in the plane, leading to structure changes in the plane of the colloidal particles. Here, a significant advantage of using soft polymer-grafted substrate is that the deformed brush provides an in-plane long-range anisotropic interaction between the colloidal particles. In Figure 3b, it is shown that the average steric energy per colloidal particle varies with increasing colloidal concentration, which clearly reflects the excluded-volume effect of colloids. As a whole, steric energy increases with increasing colloidal concentration ψ_c. Interestingly, we find that the slope of the curve has apparent differences in different ranges of ψ_c. Particularly in the region $\psi_c \approx 0.32-0.38$, where the morphology inclines to adopt hexagonal or mixed square-hexagonal structure, the slope is distinctly lower than that in other regions. This means that the steric energy can be released by forming hexagonal or mixed hexagonal-square structures.

Further, we also observe the appearance of layering transitions with increases of the effective film thickness via decreasing the height of polymer brushes. The effective thickness of the film can be defined by subtracting the brush height from the distance L_z between two substrates, i.e., $d_{eff} = L_z - 2h$, where the dry brush height h satisfies $h = \sigma N/\rho_0$ in the incompressible system of brush and homopolymer molecules.[48] Thus, the effective thickness d_{eff} of the film is changeable and increases with decreasing polymer-grafted density σ. Figure 4 shows the

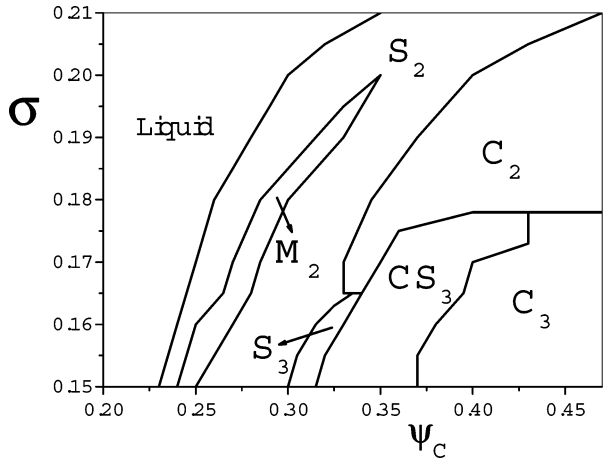

Figure 5. Phase diagram as a function of the grafting density and the colloidal concentration. S_2, two-layer sparse or dense square structure; M_2, two-layer hexagonal or mixed square-hexagonal structure; C_2, two-layer cylindrical structure; S_3, three-layer spherical structure; CS_3, three-layer cylindrical-spherical mixed structure; C_3, three-layer cylindrical structure.

possible three-layer structures such as mixed spherical-cylindrical, complete cylindrical, and even spherical structures for the selected values of σ and ψ_c. To clarify the phase stability of different ordering structures,[49] we calculate the phase diagram as functions of the grafting density and the colloidal concentration, as shown in Figure 5. Here, we choose the grafting density σ within the range 0.15−0.21 for two reasons: on one hand, the entropic change of deformed brushes should be large enough to cause effective brush-mediated interaction between colloids, requiring that the value of σ cannot be too small; on the other hand, the effective film thickness should be thick enough (namely σ is reasonably small) to ensure the possibility of colloidal crystallization. We see from Figure 5 that, when the grafting density is relatively large, the two-layer colloidal structure can be disordered liquid, square, or cylindrical. In this case, the brush-mediated interaction always dominates, which drives the self-assembly of colloids into a square lattice at small ψ_c and cylindrical structure at larger ψ_c. The hexagonal phase disappears at the middle concentrations of colloids. For intermediate values of polymer-grafted densities ($\sigma = 0.21-0.18$), the two-layer structure remains unchanged, but a reentrant structure transition between sparse square → hexagonal (or square-hexagonal) → dense square lattice structures appears as a result of the competition between brush-mediated interaction and steric packing effects of colloids. When $\sigma < 0.18$, layering transition may appear for sufficiently large values of ψ_c. The three-layer spherical-cylindrical structure (CS_3 phase) appears

(48) Matsen, M. W. *J. Chem. Phys.* **2005**, *122*, 144904.

(49) To search the stable phases of the film, we first ascertain the symmetries of possible structure formation and then calculate the free energy of the film. Furthermore, the total free energy minimization of the system with respect to the selected simulation sizes is required; this is accomplished by adjusting the lateral dimension.[46]

first, where cylindrical structures closing to brush surfaces are formed because of colloidal particles favoring the aggregation onto brush surfaces at first, and the middle layer still retains discrete spherical structure. With increasing colloidal concentration, the cylinder-forming monolayer becomes a template which drives the ordering of other colloidal particles in the middle of the film with the help of the deformation of free polymers in the suspension, and then the three-layer cylindrical structure (C_3) appears. If σ is decreased below 0.165, three-layer spherical structure (S_3 phase) may be formed for intermediate ranges of ψ_c, before the appearance of mixed spherical-cylindrical structures. The phase diagram shown in Figure 5 also provides useful information about other structural changes of the system. For example, one can observe the structural and layering transitions with increasing effective film thickness (equivalently expanding the distance between the two plates) via decreasing grafting density σ for fixed colloidal concentration ψ_c. If one changes the distance between the two plates while increasing the colloidal concentration, the colloidal structural transitions can be obtained along a tilted direction from left to right in Figure 5.

Conclusions

We study the phase behavior in thin films of confined colloid−polymer mixtures. Depending on the competition between brush-mediated interaction and steric packing effects of colloids, the colloidal self-assembly can experience a series of in-layer symmetry-changing transitions between square lattice, hexagonal, and cylindrical structures, which can be induced by changing the colloidal concentration. Furthermore, the layering transitions can be obtained by changing the film thickness of the system. We find that the colloidal particles lying on the polymer brush form a monolayer, in which the deformed chains produce an in-plane long-range anisotropic interaction that controls the ordering of the colloidal particles. This layer of ordered particles then becomes a template on which the other colloidal particles in the middle of the film grow into a large ordered structure with the help of free polymers in the region. The results may provide a helpful guide for fabricating the functionally useful microstructures in materials science of complex liquids. The suggested approach is also suitable for understanding colloidal self-assembling on other soft walls, such as the packing of biomacromolecules confined within biomembranes.

Acknowledgment. This work was supported by the National Natural Science Foundation of China, Nos. 10334020, 10021001, 20490220, and 10574061.

JA057569Q